# Studies of Multiple Scattering Effects in the Measurement of Spacial Resolution for Muon Detectors

Theodore Tomalty

McGill University

theo@tomalty.com

**Abstract**

*The McGill ATLAS Group will be testing and characterizing all muon detectors built in Canada to be installed in the ATLAS detector during the 2018 LHC shutdown. Part of the testing process requires an evaluation of the spatial resolution of each detector for the purposes of quality assurance. These measurements are to be performed using cosmic ray muons. The goal of this project is to quantify the effect of muon multiple scattering on the spatial resolution measurements. For expected spatial resolution of order 100um, and using data from simulated apparatus and interactions, the multiple scattering of cosmic muons is observed to worsen this measured spatial resolution by approximately 1%. Therefore, the measurement of the detectors' spatial resolution will not be limited by multiple scattering effects and will provide a meaningful measure of each detector's performance.*

## I Introduction

The McGill ATLAS Project is tasked with testing and characterizing numerous muon detectors that will be made across Canada and installed in the ATLAS detector, at CERN, during the 2018 LHC shutdown. Each detector, or quadruplet, is composed of four planar ionization chambers, Thin Gap Chambers (TGCs). A TGC measures the horizontal position of a passing charged particle. The measurements of all four TGCs in the quadruplet are used to reconstruct the trajectory of the passing particle. Within the testing procedure, part of determining the effectiveness of a quadruplet requires measuring the resolution of its component TGCs.

As these quadruplets will be installed in the Small Wheel of the ATLAS detector they are trapezoidal in shape (see fig. 9) in order to fit side-by-side into a rough disk. The primary objective of these detectors will be to measure the muon angles relative to the collider axis, which means that only the $y$-component of the positions (the radial positions in the Small Wheel) will be measured precisely.

The setup at McGill's testing facility comprises of an array of detectors placed horizontally between two triggering scintillators. The detectors take measurements of the positions of cosmic ray muons and the resolution of the detectors will be found by observing how closely those measurements follow a straight line.

More precisely, inclusive residuals are found by fitted a straight track through the four points and measuring the $y$-deviations between the hit and track within an individual layer. Exclusive residuals are found by repeating the above procedure but only considering three points for the track fit (all points that are not being compared to the fit). The square of the resolution of an individual layer can then be calculated as the product of the widths of the inclusive and exclusive residual distributions for that layer [2].

The trouble with the above approach is that muons do not follow perfectly straight lines in a detector. Rather, they experience Coulomb scattering from interacting electromagnetically with the medium they pass through. Thus, in order to measure the true resolution of the detectors it is important to quantify the effect of this multiple scattering on the residual distributions described above.

## II Simulation

Since the true positions of the muons can not be known using the quadruplets themselves, the entirety of this project uses data generated by CERN's Geant4 simulation software. The simulation included five stacked quadruplets, spaced evenly by 45cm. Each quadruplet was composed of layers of plastic, gas, and metals, with thicknesses corresponding to the actual construction of muon detectors, described in table 1. Two scintillators were also placed on either side of the array with properties described by table 2.

### 2.1 Muon Spectrum

It is imperative to know, as accurately as possible, the energy and angle spectrum of muons that will be measured by the detectors. As we will see, the degree of multiple scattering will depend heavily on these quantities. Unfortunately, the spectrum can not be measured in the lab itself, so it must be approximated using information that is known.

Kempa and Brancus [3] take results from many experiments and approximate the vertical muon energy spectrum at sea-level with a parabola in log-log space given by equation 1, where $p_\mu$ is the momentum in GeV/c$^2$ and $I_0$ is the probability density. In addition, several papers such as that of Bektasoglu and Arslan [4] suggest that the zenith angle distribution of muons follows a *cos n* law, given by equation 2, where $\phi$ is the zenith angle.

$$\begin{aligned} \log(I_0) &= a\ln^2(p_\mu) + b\ln(p_\mu) + c \\ a &= -0.1292 \pm 0.0005 \\ b &= -0.266 \pm 0.002 \\ c &= -2.600 \pm 0.003 \end{aligned} \tag{1}$$

$$\begin{aligned} I &= I_0 \cos^n(\phi) \\ n &= 1.95 \pm 0.08 \end{aligned} \tag{2}$$

The lab, which is at approximately sea-level, is on the second floor of McGill's Rutherford building. Therefore the 2m of concrete that rests above the detectors must be accounted for in the effective muon spectrum (this is a very rough estimate found by looking at walls in the stairwell.) To study this effect, muons were simulated with the sea-level spectrum described above (see fig. 10), passed through 2m concrete, and the attenuated spectrum was recorded in figure 11. The spectrum from this histogram could then used to generate muons to appear in the experiment.

## III Multiple Scattering

Multiple scattering is the process by which a particle's trajectory is altered due to interactions with the medium it passes through. For charged particles, scattering comes primarily from Coulomb Scattering, which is the result of electromagnetic interactions.

### 3.1 The Molière Model

The Molière model of Coulomb Scattering predicts the change in angle of a particle as it passes through a certain amount of material. The scattering angle is defined as the 2D change in angle that a charged particle undergoes as it passes through a certain distance of a given material. To get a 2D angle from three dimensional "before" and "after" momentum vectors, one must project the momentum vectors onto any plane containing the incident track, and then measure the angle between the projected vectors.

According to the model, the scattering angle measured in any such plane, will be Gaussian distributed with standard deviation given by equation 3, where $p$ is the muon's momentum, $\beta c$ is the velocity of the muon, $x$ is the distance traversed by the muon, $X_0$ is the radiation length of the medium, and $\alpha = 0.038$ [1].

$$\sigma_\theta = \frac{13.6 \text{ MeV}}{\beta pc}\sqrt{\frac{x}{X_0}}\left[1 + \alpha \log\left(\frac{x}{X_0}\right)\right] \tag{3}$$

The radiation length of a material, $X_0$, is the distance over which a charged particle will have its energy reduced by a factor of $e^{-1}$. A detector that is composed of many different materials, however, does not have a definite radiation length. Instead, a muon passing through will traverse $N$ radiation lengths in the sense that its energy will be reduced by a factor of $e^{-N}$.

For a muon passing perpendicularly through a quadruplet, the $N$ of the entire detector is simply the sum the contributions from individual materials $N_i = \frac{x_i}{X_0^i}$, where $x_i$ is the thickness of a single material and $X_0^i$ is the radiation length of that material. If, however, the muon is entering the detector with a certain angle of incidence, $\phi$, then the distance travelled within each material will increase by a factor of $1/\cos(\phi)$. Therefore, the quantity $x/X_0$ in equation 3 is equivalent to $N/\cos(\phi)$ where $N$ is the number of radiation lengths traversed by a perpendicular muon, which is independent of the particle's properties.

### Results

With a given detector geometry and composition (see table 1), the width of the Gaussian scattering angle distribution, $\sigma_\theta$, becomes a function of energy and incident angle only. Taking muons with a few combinations of those quantities, one can compare the distribution of scattering angle measurements from the simulation with the distribution predicted by the Molière Moodel (see fig. 13).

It becomes clear that there is good agreement between the simulation and the model. However, by showing the same results in a log scale, in figure 14, one notices that the tails of the histograms are larger than those predicted by the model. This is due to Rutherford Scattering, which is a less frequent, but more violent type of interaction with the medium.

In order to verify the validity of equation 3 over a continuum of energies and incident angles, each quantity was varied independently. The data was separated into bins of the varying quantity. A histogram of the scattering angle distribution was made using muons from each bin and fitted to a Gaussian function. The RMS of the best fit Gaussian was found for each bin and plotted versus total energy and incident angle (bin centres of the varying quantity) in figures 17 and 18 respectively.

The solid line in both of the above figures represent a constant factor fit of equation 3 to the data. As one can see from the ratio plots at the bottom of both figures, the results matched the model very well with only a shift of about 1% in the plot versus energy. This was a reasonable shift since, according to the Particle Data Group [1], equation 3 is accurate to $\pm 2\%$ depending on the range of the Gaussian function that is fitted to the scattering angle distribution.

## 3.2 Deriving a Distance Quantity

The goal of this project is ultimately to compare residual distributions due to multiple scattering with residuals due to detector resolution. To that end, we will attempt to characterize multiple scattering using a quantity that behaves like a "spacial error" of sorts. Although this quantity could be any number of observables, we will use the scattering error, to be defined, because it makes intuitive sense and because it will work well in the later sections.

Recall that Molière gives a model for the scattering angle as a particle passes through material, projected onto some plane that contains the incident trajectory of the muon. Equation 3 gives the RMS of the scattering angle distribution for some fixed plane. We define the perpendicular distance of the muon as the distance between the muon's position, projected onto the same fixed plane, and the linear extrapolation of the muon's initial trajectory. According to the PDG, the perpendicular distance of the muon is Gaussian distributed with RMS given by equation 4, where $x$ is the distance traversed by the particle and $\sigma_\theta$ is the RMS of the scattering angle distribution predicted by equation 3.

$$\sigma_{\text{perp}} = \frac{x}{\sqrt{3}}\sigma_\theta(E, \phi, N) \qquad (4)$$

Note that equation 4 does not depend on

the plane onto which the muon position is projected (as long as the plane contains the initial trajectory of the muon). One can, therefore, consider a perpendicular plane that is normal to the muon's incident trajectory, where the origin coincides with the linearly extrapolated trajectory. The intersection of the true path of the muon with the perpendicular plane, after multiple scattering effects, is given by a 2D Gaussian distribution whose width corresponds to equation 4. In that case, $x$ is the distance between the origin of the perpendicular plane and the "point of entry".

We now define scattering distance the the $y$ position of a muon in a given TGC relative to what the position would have been if the muon had continued in a straight line from its position in the previous layer. In other words, if the state of a muon in one of the TGC layers is known, the scattering distance is a measure of how much multiple scattering affected the $y$ position of the particle in the next layer.

The perpendicular distance relates back to scattering distance when we consider the "point of entry" being given by the position and direction of the muon in a particular TGC. We then look at the 2D Gaussian distribution of the particle's position in the perpendicular plane who's origin coincides with the next layer. The width of the 2D Gaussian in the perpendicular plane is given by equation 4, where $\phi$ is the incidence angle, $x = \text{width}/\cos(\phi)$ is the distance traversed between the TGC detection layers, $N$ is the number of radiation lengths between the two layers, and $E$ is the initial energy of the particle.

We want the width of the position distribution of the muon along the $y$ axis of some TGC, not along some axis that is perpendicular to the incident direction of the muon. Therefore, the 2D Gaussian position distribution in the perpendicular plane must be projected onto the horizontal plane of the given TGC along the extrapolated trajectory of the muon. The distribution of scattering distance can finally be found by collapsing the projected distribution onto the $y$ axis

To project the 2D Gaussian perpendicular distance distribution onto the horizontal plane we simply elongate the distribution by $1/\cos(\phi)$ in Azimuthal direction of the incident muon. The RMS of the collapsed distribution in $y$ is $\sigma_{\text{perp}}$ multiplied by a projecting factor given by equation 5. This represents the RMS of the elongated and non-elongated components of the horizontal distribution projected onto the $y$ axis, where $\psi$ is the azimuth angle measured counterclockwise from the $x$-axis

$$\gamma(\phi, \psi) = \sqrt{\cos^2(\psi) + \frac{\sin^2(\psi)}{\cos^2(\phi)}} \tag{5}$$

The collapsed distribution in $y$ represents the distribution of scattering distance. We call the predicted width of this distribution the scattering error, $\sigma_S$, and it is expressed by equation 6. Since $E$ and $\phi$ do not vary much within a detector, this quantity is constant for a given muon and represents spacial deviation in detection layers due to multiple scattering effects.

$$\sigma_{\text{S}} = \gamma(\phi, \psi) \frac{x_{\text{layer}}}{\sqrt{3}\cos(\phi)} \sigma_\theta(E, \phi, N_{\text{layer}}) \tag{6}$$

## Results

Taking a similar approach as in section 3.1, the normalized distributions of multiple scattering distance were plotted in figure 15 for a few combinations of energy and incidence angle. A fixed azimuth angle of $\psi = \frac{\pi}{4}$ was used for simplicity. The overlapping Gaussian functions, with RMS given by equation 6, represent the predictions of the model derived above. One can observe, however, a much better approximation of the data from figure 16 which uses a double Gaussian fit.

The energy and incidence angle of the muons were varied independently. In bins of the varying quantity, the scattering distance distribution was found and fitted to a double Gaussian. The RMS of the combined Gaussians were plotted in figures 1 and 2 for varying energy and incidence angle respectively. Here, the RMS of the sum of two Gaussians is found using equation 7, where $A$ and $B$ are the amplitudes of the first and second Gaussian and $\sigma_1$ and $\sigma_2$ are their respective standard deviations.

$$\sigma_S = \frac{A\sigma_1^3 + B\sigma_2^3}{A\sigma_1 + B\sigma_2} \tag{7}$$

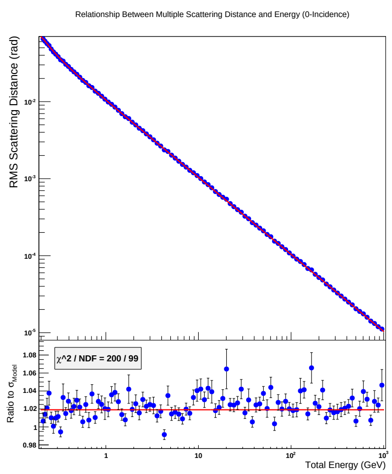


**Figure 1:** *The RMS of multiple scattering distance distribution for zero incidence muons versus muon energy. The data was fitted to a constant factor of the model prediction in equation 6.*

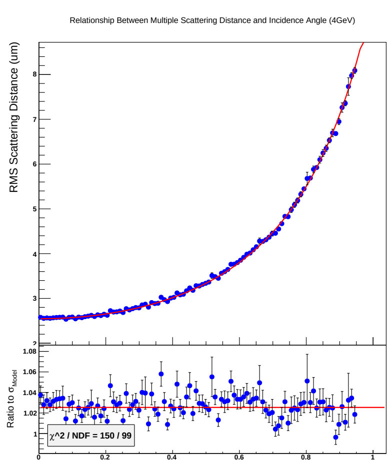


**Figure 2:** *The RMS of multiple scattering distance distribution for 4GeV muons versus zenith angle ($\frac{\pi}{4}$ azimuth angle). The data was fitted to a constant factor of the model prediction in equation 6.*

One may note that the RMS of the scattering distance is shifted systematically from the model prediction by roughly 2%. This, however, is understandable since the RMS of a double Gaussion fit is skewed more by Rutherford scattering than a single Gaussian would be, due to the increased number of degrees of freedom.

## 3.3 Modelling Scattering Residuals

Using the understanding of multiple scattering developed so far, we can attempt to understand how multiple scattering is related to residuals. For particles entering the detector with a given energy and incident angle, we will attempt to construct a model for the residual distribution that they create. For the time being, detector resolution is assumed to be perfect.

Residuals have units of distance, as they measure the deviation between the measured $y$ position of a muon to that of a straight track. From intuition, the width of a residual distribution for a given layer represents a positional uncertainty of sorts, as the scattering error does. It, therefore, does not take a leap of reasoning to imagine that the two quantities in equation 8 are proportional to each other.

$$\sigma_{\text{residual}} = a\sigma_S \tag{8}$$

We consider zero-incidence muons with varying energy separated into bins of scattering error (Recall that this quantity was calculated uniquely for a given muon using equation 6). A Gaussian function was fitted to the residual distribution of muons in each bin, and the RMS of the fits were plotted as a function of bin centre in figure 3. The data are very clearly increasing linearly, which demonstrates the proportionality that was predicted above.

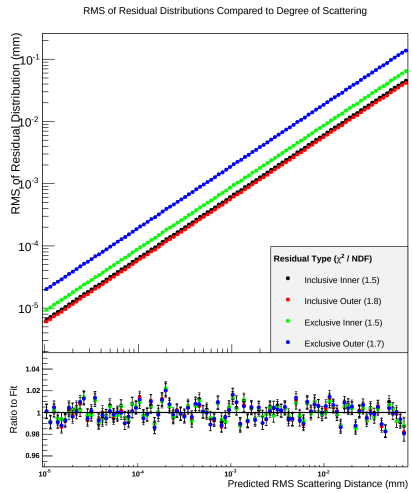


**Figure 3:** *The RMS of Gaussian residual distributions in bins of scattering error (calculated using equation 6) for zero incidence muons and varying energy. Slopes of fit lines recorded in the a-column of table 3.*

## 3.4 Expected Scattering Residuals

At the end of the day, the expected residual distribution for a perfect detector is given by figure 4. These distributions were measured using the positions of simulated muons in all 5 quadruplets. The muons began with an attenuated sea-level spectrum given by figure 11 distributed evenly on the surface of the top scintillator, and were only considered if they hit both scintillators.

In order to model the final residual distribution in figure 4, equation 8 was integrated over the spectrum of muons in the apparatus. More precisely, the energy, zentih angle, and azimuth angle spectrum was collapsed into a scattering error spectrum using equation 6 (the projection of figure 12 onto the scattering axis). The total residual distribution is modelled as the sum of Gaussians over the bins of that spectrum — Gaussians with RMS given by equation 8 with area weighted by the bin size.

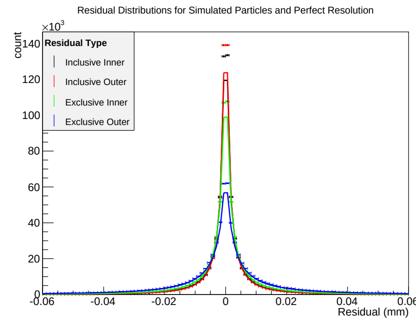


**Figure 4:** *The residual distributions for attenuated sea-level muons with multiple scattering effects and perfect detector resolution.*

# IV Detector Resolution

The spacial resolution of a given TGCs determines how precisely it can measure the position of passing muons. Due to a similar construction of each TGC and quadruplet, we assume that the resolution of each layer is identical. In the simulation, resolution is modelled by adding a Gaussian distributed random number to each true position with RMS equal to the detector resolution.

From test beam results of quadruplets that are now in employment [5], it is clear that the resolution of the strips channel (i.e. resolution in the $y$-direction) follows a linear relationship with the incident angle of the muons. Indeed, a muon that enters at a nonzero angle will deposit energy in a larger region of the gas volume than if it had entered perpendicularly. The component of the moun's velocity the $x$-direction, however, should have no effect on the width of the energy distribution in the $y$-direction, so the $y$-resolution should be a function of the incidence angle projected onto the $y$-axis only, described by equation 9.

$$\sigma_y = a\theta_y + b \tag{9}$$

To coincide roughly with the detector resolutions measured in test beam, we used $a = 0.27\text{mm/rad}$ and $b = 0.060\text{mm}$. It is important to note, however, that these values are a ballpark estimate of detector resolution, as in reality it will depend on many things like the voltage of the strips and the fidelity of the channels.

### 4.1 Modelling Resolution Residuals

In this section we assume that multiple scattering is negligible. A muon will follow a straight path through the detector, and the residuals arise from imprecision in the measurements due to detector resolution.

According to Carnegie *et. al.*, the width of the residual distributions can be statistically calculated given a certain detector geometry and resolution [2]. These distributions are Gaussian with RMS given by equation 10 where the $b$ values are written explicitly in table 3. Note that the coefficients do not depend on the spacing of the TGC layers nor incident angle of the muons.

$$\sigma_{\text{residual}} = b\sigma_y \tag{10}$$

Indeed, for zero-incidence muons following straight lines, detector resolution was incremented and for each resolution the RMS of the Gaussian residual distribution was plotted in figure 5. The solid lines show the prediction of equation 10, and are in good agreement with the data.

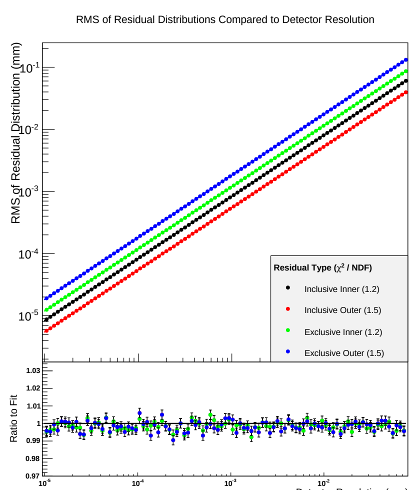


**Figure 5:** *The RMS of Gaussian residual distributions versus detector resolutions (neglecting scattering). Fixed lines, using slopes in the b-column of table 4.*

### 4.2 Expected Resolution Residuals

Figure 6 depicts the residual distributions for attenuated sea-level muons, that do not scatter, with detector resolution following equation 9. The residual distribution were modelled by integrating Gaussians with RMS given by equation 10 over the spectrum of detector resolution (fig. 12 projected onto the resolution axis).

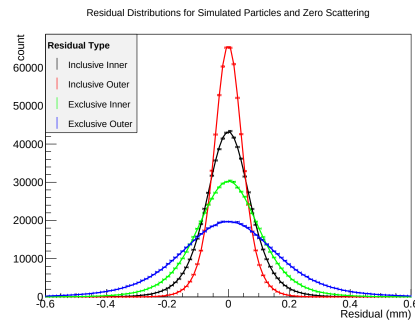


**Figure 6:** *The residual distributions for attenuated sea-level muons with detector resolution effects and without multiple scattering.*

## V Convolution of Effects

We have now constructed models that predict the behaviour of residuals when either multiple scattering or detector resolution is negligible. Residuals in reality, however, form as a convolution of the two effects.

A preliminary guess as to the the width of the residual distributions when both effects are taken into account would be to add the width of residuals from only scattering and only resolution in quadrature. However, due to the differing nature of the two effects, equation 11 also employs a combined term that is only significant when both effects have the same order of magnitude.

$$\sigma_{\text{residual}} = \sqrt{(a\sigma_S)^2 + (b\sigma_y)^2 + 2c\sigma_S\sigma_y} \tag{11}$$

The values of $a$ and $b$ should correspond to the slopes when $\sigma_y$ and $\sigma_S$ are negligible respectively, shown in table 3 as a result of the earlier analysis. The widths of the inclusive residual distributions, on inner layers, are plotted in figure 7 as a function of resolution and scattering error. The scattering error was varied by manipulating the incoming muon energy, holding the incidence angle fixed at zero. Equation 11 was fitted to the data, with $a$, $b$, and $c$ as fit parameters.

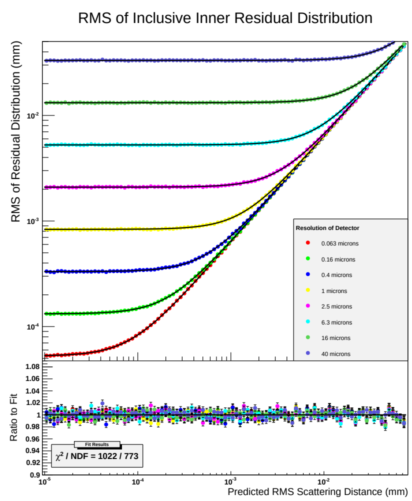


**Figure 7:** *The RMS of Gaussian residual distributions in bins of scattering error (calculated using equation 6) for zero incidence muons and varying energy. Data sets were constructed using different (fixed) detector resolutions. The data are fitted to equation 11, with a, b, and c as fit parameters recorded in table 4.*

The same method was used to evaluate $a$, $b$, and $c$ for the other residual distributions, and the results were recorded in table 4. One may compare values for $a$ and $b$ in table 4 and table 3 to find a general 0.5% agreement.

We then measure the final residual distributions in figure 8, taking into account both multiple scattering and detector resolution with our attenuated spectrum of muons. It is modelled by integrating Gaussians, with RMS given by equation 11, over the spectrum of scattering error and detector resolution given by figure 12.

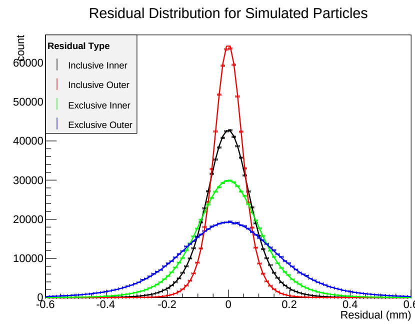


**Figure 8:** *The residual distributions for attenuated sea-level muons with both scattering and resolution effects.*

## VI Conclusion

The purpose of this project was to determine the degree to which multiple scattering will affect the residual distributions of the TGCs, and the measured resolution by extension. We, therefore, compare the widths of the residual distributions in figures 8 and 6, in table 5, to get a shift of about 1-2% between residual distributions with and without scattering.

Since resolution squared is measured as the product of inclusive and exclusive residual widths (with some constant factor), this equates to a shift in measured resolution of 0.78% and 1.24% for inner and outer layers respectively.

This result is appropriate for resolutions on the order of 100 microns, while higher orders would see a decrease in percent difference. It, therefore, becomes clear that multiple scattering of cosmic ray muons is a minor contributor to the residual distributions that will be observed at McGill's facilities.

## References

[1] K. A. Olive *et al.* [Particle Data Group Collaboration], Chin. Phys. C **38**, 090001 (2014). **27.3. Multiple scattering through small angles**

[2] R. K. Carnegie *et al.* NIM A538 (2005) 372-383. **Resolution studies of cosmic-ray tracks in a TPC with GEM readout**

[3] J. Kempa and I. M. Brancus (2003), "Zenith angle distributions of cosmic ray muons", Nuclear Physics B (Proc. Suppl.) 122, pp. 279-281

[4] M. Bektasoglu and H. Arslan (2013), "Investigation of the zenith angle dependence of cosmic-ray muons at sea level", Pramana 80, pp. 837.

[5] J. Yu (2013), "Test beam and simulation studies on thin gap chambers", University of Michigan.

# VII Appendix

| Material | Width (mm) | Radiation Length (mm) |
|---|---|---|
| Plastic | 1.4 | 425.4 |
| Copper | 0.03 | 14.36 |
| Carbon | 0.05 | 213.5 |
| Tungsten | 0.004 | 3.504 |
| TGC Gas | 1.348 | 308050 |
| Aluminum | 5.0 | 2001 |
| Totals | " | N |
| Layer | 10.92 | 0.01953 |
| Quad | 48.68 | 0.08061 |

**Table 1:** *Materials and Geometry of a Quadruplet. 4 TGCs are contained between aluminum honeycomb layers, one on top and one on the bottom of the quadruplet, as well as one layer between each TGC. Each TGC is then composed with layers of copper, plastic, copper, 0.1mm plastic, carbon, gas, tungsten, and the same thing, excluding tungsten, in reverse order.*

| Material | PLASTIC_SC_VINYLTOLUENE |
|---|---|
| Thickness ($z$) | 3.0 cm |
| Length ($x$) | 3.2 m |
| Width ($y$) | 1.2 m |
| Spacing | 2.064 m |

**Table 2:** *Geometry and material of the scintillators in the test bench used for simulation. The dimensions represent the full lenghts, and spacing is measured from the bottom of the top scintillator to the top of the bottom scintillator.*

| Residual Distribution | $a$ | $b$ |
|---|---|---|
| inclusive inner | $0.6317 \pm 0.0004$ | $\sqrt{0.7}$ |
| inclusive outer | $0.5845 \pm 0.0003$ | $\sqrt{0.3}$ |
| exclusive inner | $0.9003 \pm 0.0005$ | $\sqrt{0.7}^{-1}$ |
| exclusive outer | $1.938 \pm 0.001$ | $\sqrt{0.3}^{-1}$ |

**Table 3:** *a and b represent the slopes of the lines in figures 3 and 5 respectively.*

| Residual Distribution | $a$ | $b$ | $c$ | $\chi^2$ | NDF |
|---|---|---|---|---|---|
| inclusive inner | 0.6294 ± 3e-4 | 0.8329 ± 3e-4 | 0.0188 ± 6e-04 | 1022 | 773 |
| inclusive outer | 0.5830 ± 3e-4 | 0.5436 ± 2e-4 | 0.0104 ± 5e-04 | 852 | 773 |
| exclusive inner | 0.8989 ± 4e-4 | 1.1899 ± 4e-4 | 0.038 ± 1e-03 | 1016 | 773 |
| exclusive outer | 1.9406 ± 8e-4 | 1.8171 ± 6e-4 | 0.122 ± 4e-03 | 1265 | 773 |

**Table 4:** *The parameters used to model residual distributions in equation 11. The first row is a result of the fit in figure 7.*

| Residual Distribution | HWHM No-scatter (mm) | HWHM With-Scatter (mm) | Percent Difference |
|---|---|---|---|
| inclusive inner | 0.08182 | 0.08276 | 1.1% |
| inclusive outer | 0.05356 | 0.05445 | 1.6% |
| exclusive inner | 0.11688 | 0.11822 | 1.1% |
| exclusive outer | 0.17855 | 0.18203 | 1.9% |

**Table 5:** *Comparing the half width at half maximum of residual distributions in figures 6 and 8.*

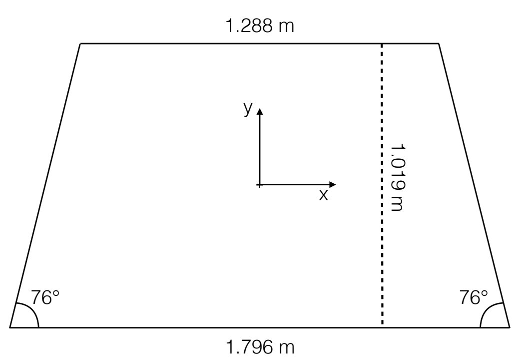


**Figure 9:** *Scaled diagram of a birds-eye view of the detector. Lengths labeled correspond to the size of the quadruplet layers in the simulation.*

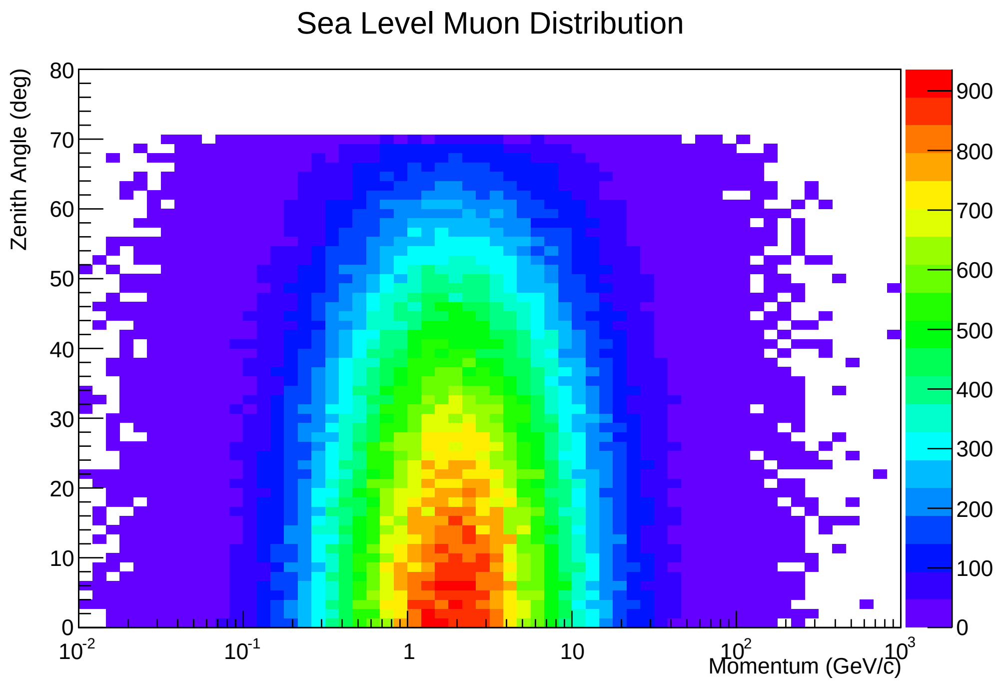


**Figure 10:** *The momentum and zenith angle distribution of muons at sea level.*

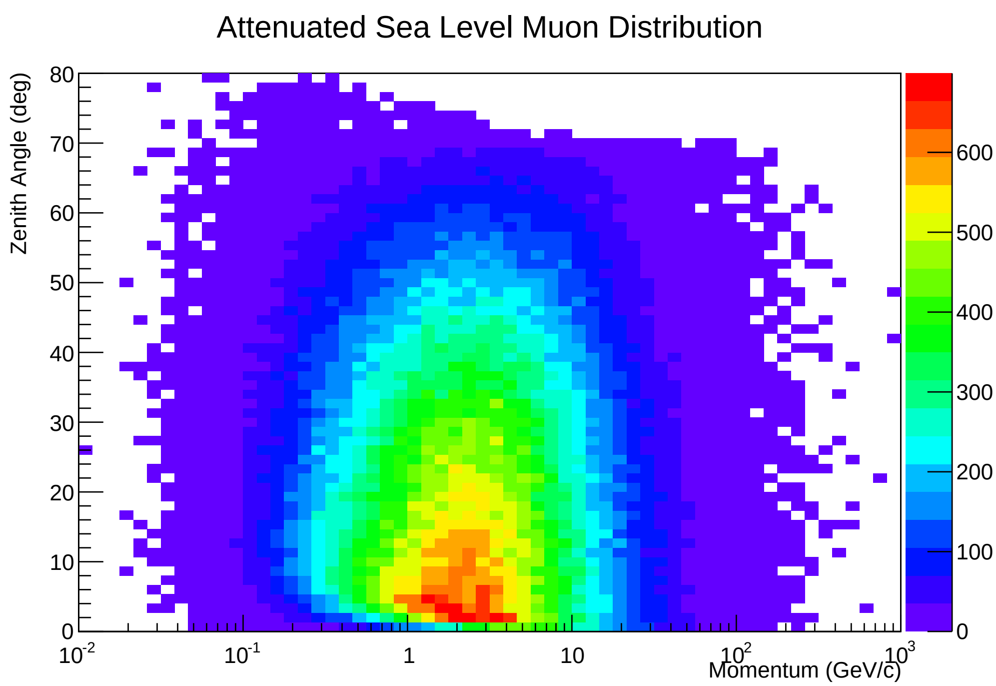


**Figure 11:** *The momentum and zenith angle distribution of muons at sea level and after passing through 2m of concrete.*

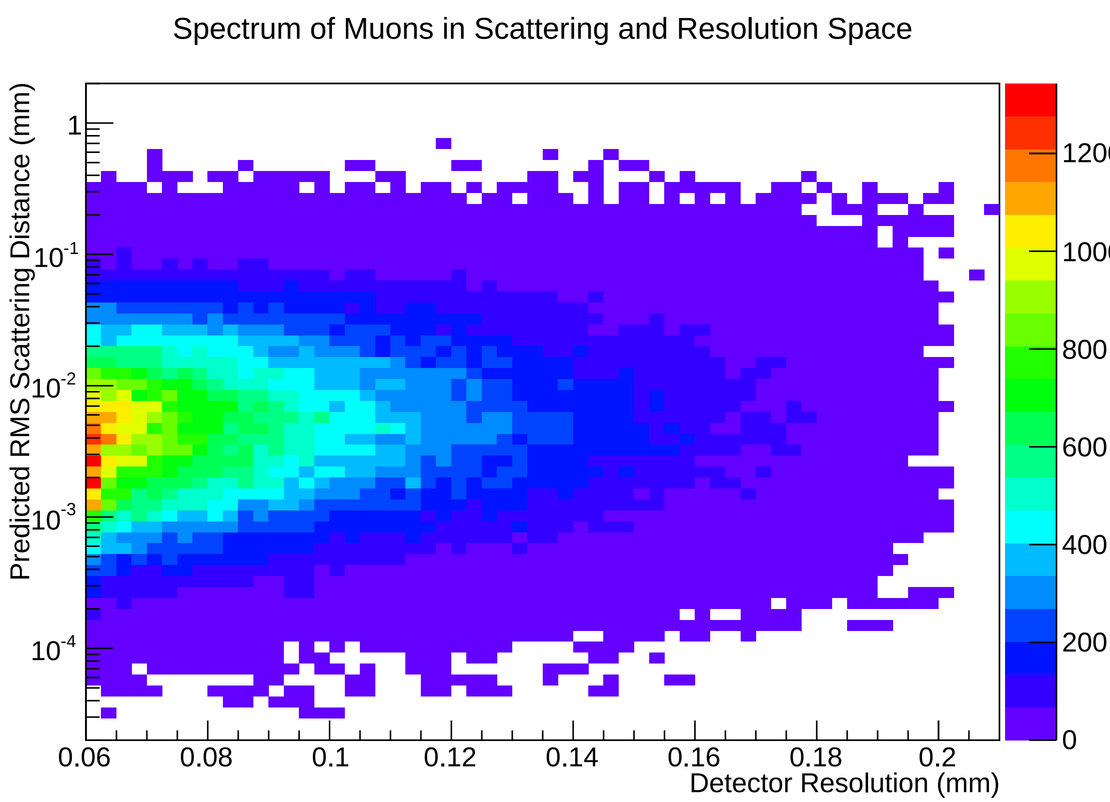


**Figure 12:** *The spectrum of muons detected by all five quadruplets in the simulation. The Predicted RMS Scattering Distance is calculated for a muon by equation 6 while Detector Resolution is found using equation 9.*

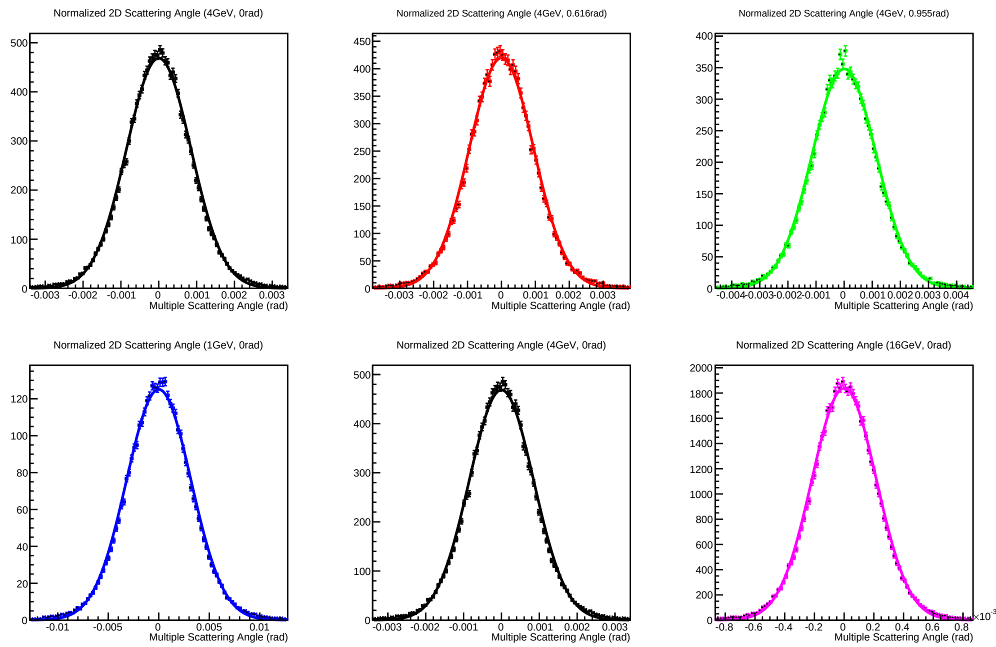


**Figure 13:** *Normalized distribution of multiple scattering angle between quadruplets, with model Gaussian. Top Row: Fixed 4GeV energy, incident angle 0rad, 0.616rad, and 0.955rad from left to right. Bottom Row: Fixed 0rad incident angle, kinetic energy 1GeV, 4GeV and 16GeV from left to right.*

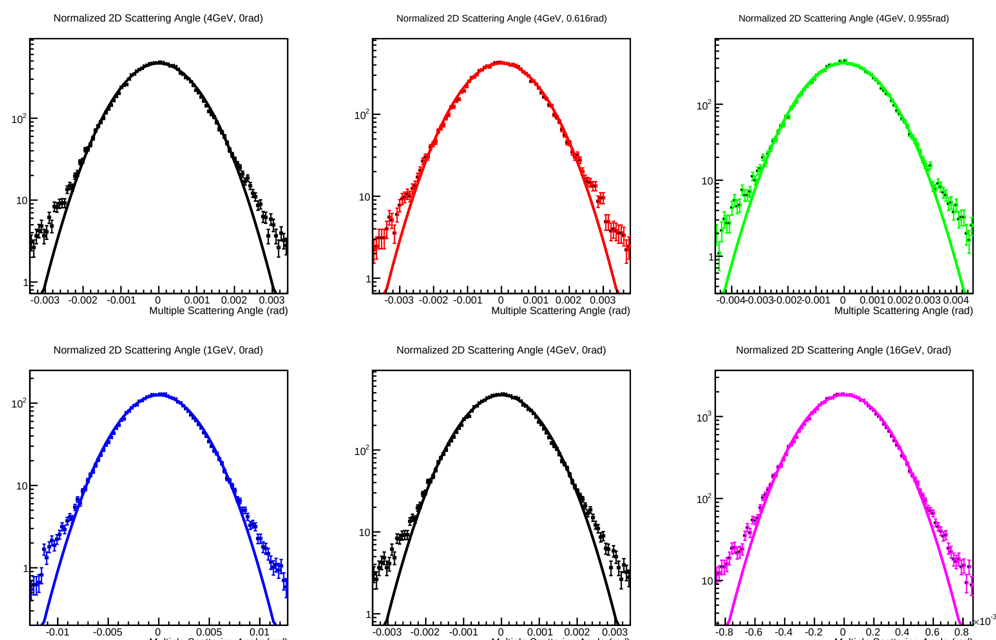


**Figure 14:** *Figure 13 with log y-axis.*

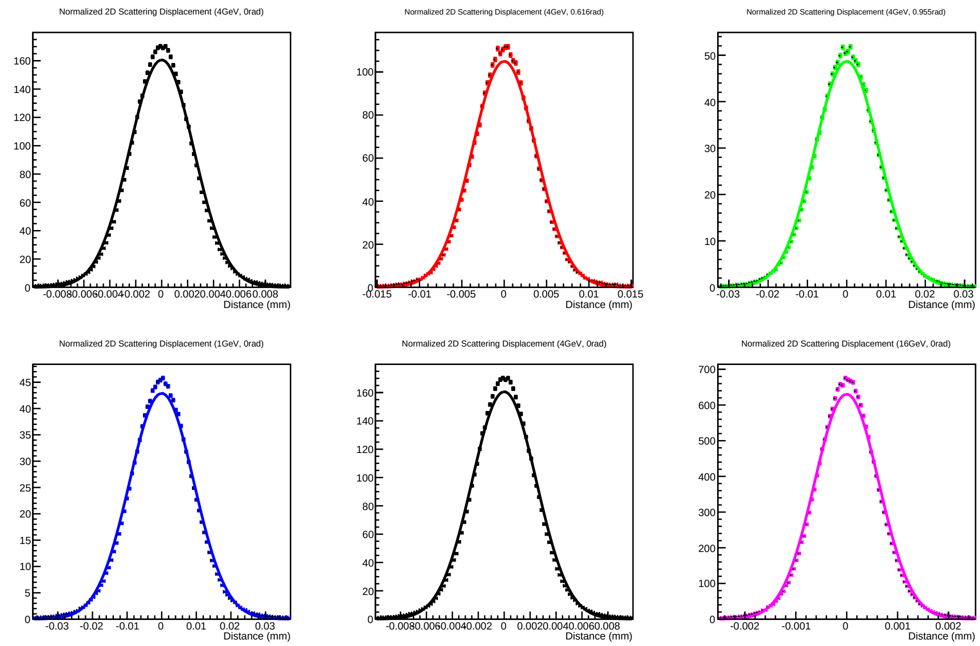


**Figure 15:** *Normalized distribution of multiple scattering distance between quadruplet layers, with model Gaussian. Top Row: Fixed 4GeV energy, incident angle 0rad, 0.616rad, and 0.955rad from left to right. Bottom Row: Fixed 0rad incident angle, kinetic energy 1GeV, 4GeV and 16GeV from left to right.*

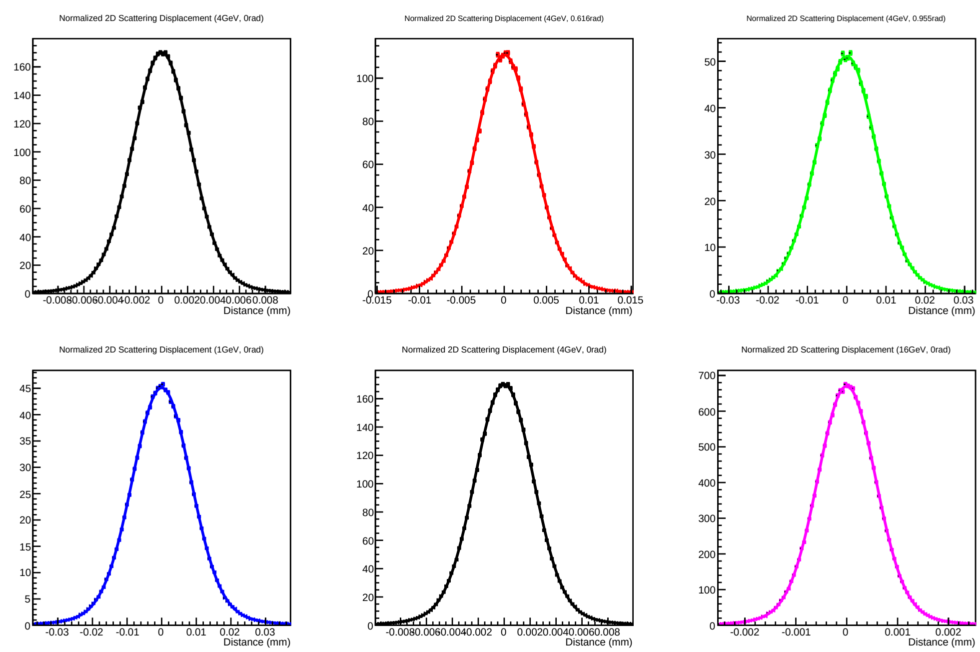


**Figure 16:** *Figure 15 using a double Gaussian fit.*

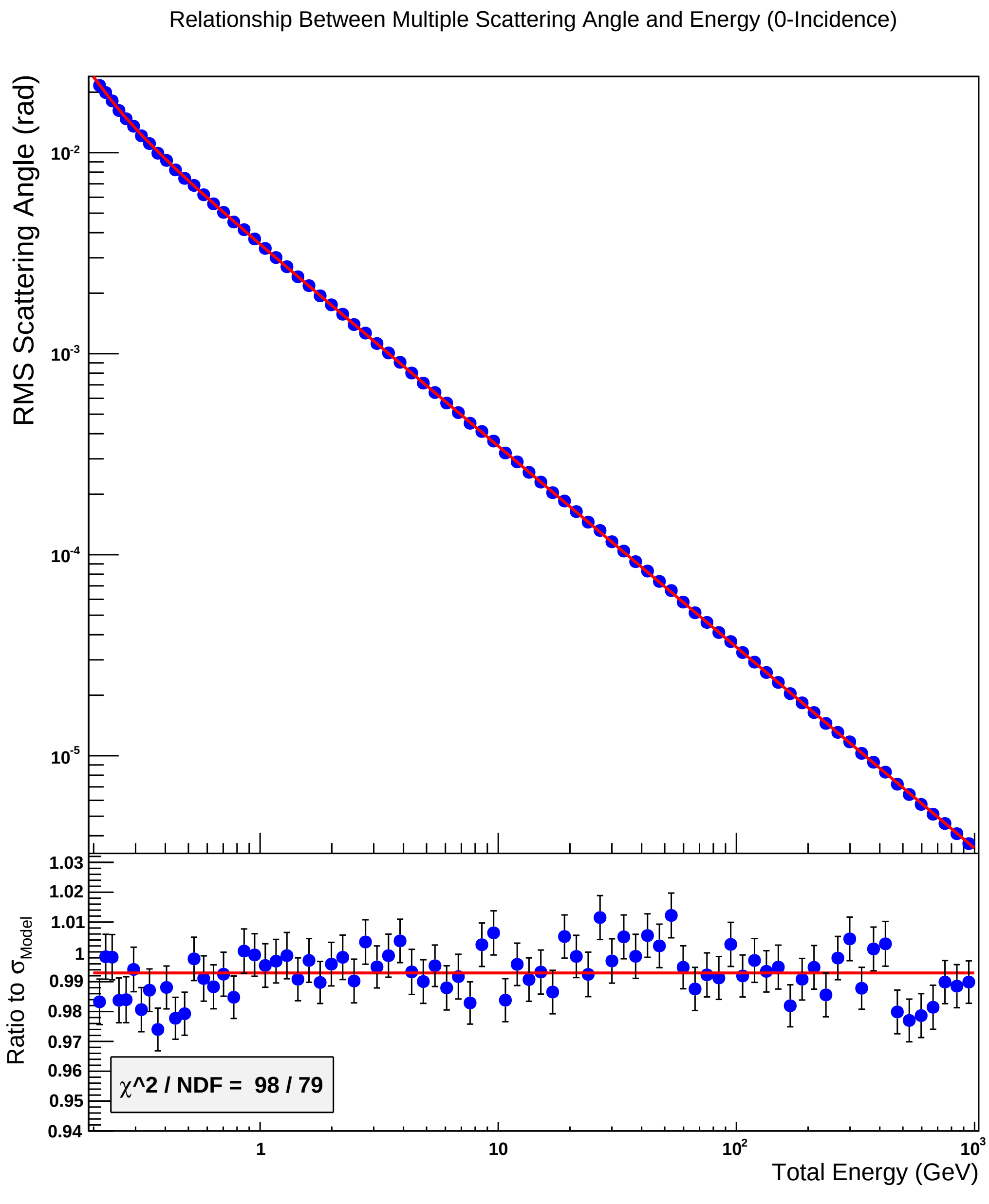


**Figure 17:** *A plot of the RMS of multiple scattering angle for 0rad incidence muons. The data was fitted to a constant factor of the model prediction by equation 3.*

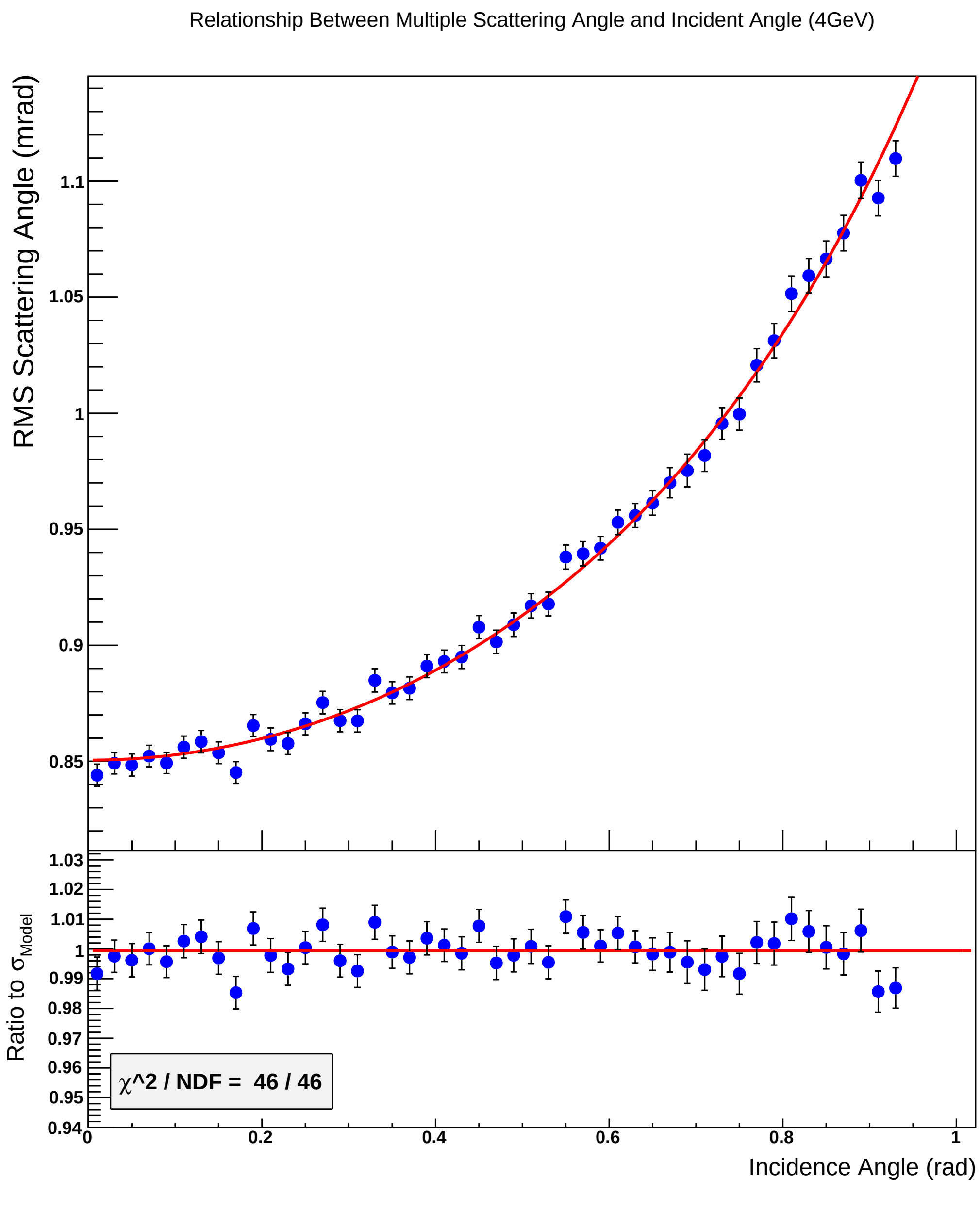


**Figure 18:** *A plot of the RMS of multiple scattering angle for 4GeV incidence muons. The data was fitted to a constant factor of the model prediction by equation 3.*